Detailed Jet Dynamics in a Collapsing Bubble

2015 J. Phys.: Conf. Ser. 656 012038

(http://iopscience.iop.org/1742-6596/656/1/012038)

Detailed Jet Dynamics in a Collapsing Bubble

Outi Supponen[1], Danail Obreschkow[2], Philippe Kobel[1] and Mohamed Farhat[1]

[1] Laboratory for Hydraulic Machines, Ecole Polytechnique Fédérale de Lausanne, Avenue de Cour 33bis, 1007 Lausanne, Switzerland
[2] International Centre for Radio Astronomy Research, University of Western Australia, M468 7 Fairway, Crawley, WA 6009, Australia

E-mail: outi.supponen@epfl.ch

Abstract. We present detailed visualizations of the micro-jet forming inside an aspherically collapsing cavitation bubble near a free surface. The high-quality visualizations of large and strongly deformed bubbles disclose so far unseen features of the dynamics inside the bubble, such as a mushroom-like flattened jet-tip, crown formation and micro-droplets. We also find that jetting near a free surface reduces the collapse time relative to the Rayleigh time.

1. Introduction

An important aspect of cavitation bubbles is their erosive power, which can be both harmful or beneficial, depending on the application. The erosion takes place during and shortly after the collapse of single bubbles, and is, in most cases, attributed to the formation of a strong shock or a fast, thin liquid jet, called the micro-jet. Such a micro-jet emerges when a cavitation bubble collapses aspherically due to anisotropies in the surrounding pressure field caused by, for example, nearby boundaries [1] or gravity [2]. The micro-jet usually becomes visible during the regrowth (rebound) of the bubble after the collapse as it pushes along a conical pocket of vapor sometimes called the vapor-jet [2]. The jet can also pierce the bubble well before the collapse when the bubble is particularly deformed [1,3]. Or, in cases of mild deformation, it might not even reach the opposite bubble wall and remains within the bubble throughout the collapse and rebound [2].

Here we study a single bubble collapsing near a free surface using high-speed imaging. This work extends on our recent visualizations of jet formation [1] and provides more quantitative insights. In the experiment (details in ref. [4]), a spherical cavitation bubble is created in water contained in a cubic ($18 \times 18 \times 18$ cm^3) test chamber. We use a green laser pulse (532 nm, 8 ns), first expanded to a diameter of 5 cm using a lens-system, and then refocussed onto a single point using a parabolic mirror with a high convergence angle (53°) to generate a point-like initial plasma [4]. In this way, we obtain a bubble of very high initial sphericity – impossible to achieve with a pure lens-system. The bubble centre is placed at a short distance of $h = 2.95$ mm below the free surface, causing the bubble to become vertically distorted during the collapse motion. This process is visualized with a high-speed camera (Photron Fastcam SA1.1) fitted with a 135 mm objective (Nikon Zoom-Micro 70–180mm f/4.5–5.6D) at a speed of 37,500 frames per second.

The experiment is conducted at room temperature and at low pressure (10.1 kPa=0.1 atm), implying large bubbles with long collapse times and thus increased spatio-temporal resolution.

2. Results and Discussion

A sequence of images showing a cavitation bubble collapsing in the vicinity of a free surface is shown in Figure 1. The bubble is initially spherical, yet upon reaching its maximum size ($R_{\max} \sim 5.3$ mm) it distorts to an egg-like shape while pushing liquid above it and deforming the free surface (frame 1 in Figure 1). The bubble then starts its collapse, during which a jet forms from the top of the bubble directed away from the free surface with a maximum speed of 8.2 m/s and an average width of 1 mm. The tip of the jet obtains an interesting "mushroom cap"-shape, which we believe is a result of interface instabilities. Figure 2 provides a more detailed visualization on the jet within the bubble, disclosing this peculiar jet shape in frames 1-4. The cap has a diameter of 2 mm. The jet then pierces the bubble well before the moment of collapse and entrains a pocket of the bubble's enclosed gases – this is the vapor-jet mentioned in Section 1. We discover that the boundary of this pocket has a complex shape, with a step leading from a diameter of 2.8 mm to 3.8 mm (frame 4 in Figure 1). These two diameters are associated with the jet and the "mushroom cap" diameters respectively. The inner part is the actual jet pushing the vapor whereas the outer part, which quickly slows down and smoothens out, is being pushed by the thin cap.

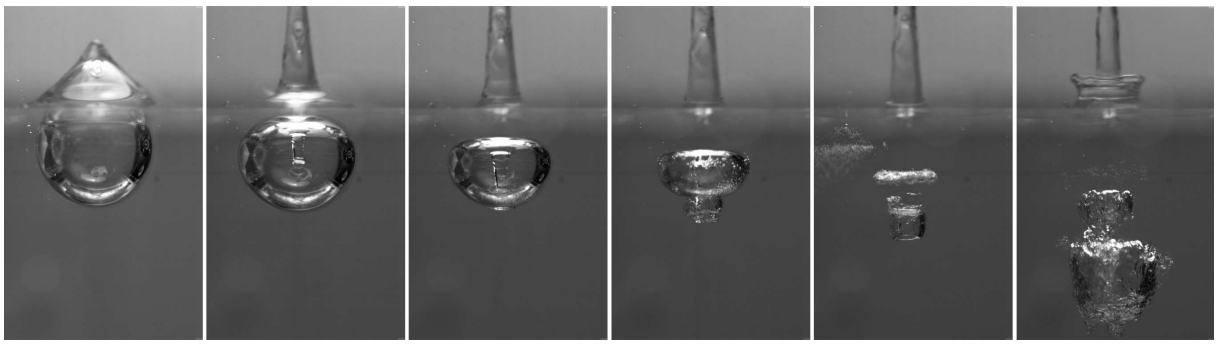

Figure 1: The collapse and rebound of a laser-induced cavitation bubble collapsing near a free surface. The frames are from times $t = 1.36, 1.96, 2.33, 2.60, 2.74$ and 3.40 ms after the bubble generation. See video in ref. [5].

The interface of the bubble quickly becomes opaque after the jet has pierced the opposite bubble wall. This is due to the shooting of micro-droplets onto the interface, which forms capillary waves on the bubble wall. These micro-droplets resulting from a crown generated within the bubble at the jet impact (frames 1-4 in Figure 2, bottom row). The jet impact occurs at spectacular Reynolds and Weber numbers ($Re \approx 10^4$ and $We \approx 10^3$ – note that the bubble interface velocity at the moment of impact is 1.5 m/s), providing conditions similar to those in investigations of a droplet impacting a flat free surface where the formation of a high-speed "ejecta"-sheet has been reported [6]. An ejecta-sheet is a thin jet that emerges rapidly after the impact horizontally between a drop and the free surface. For a sufficiently energetic impact ($We > 500$) this sheet disintegrates into tiny droplets [7].

The ejected micro-droplets mainly perturb the bubble boundary in the lower part of the bubble, near the impact point (last frame in Figure 3). However, as the collapse of the bubble continues, every point of its surface gets eventually sucked into the jet as shown theoretically in ref. [8]. By this process, the capillary surface perturbations that formed at the bottom of

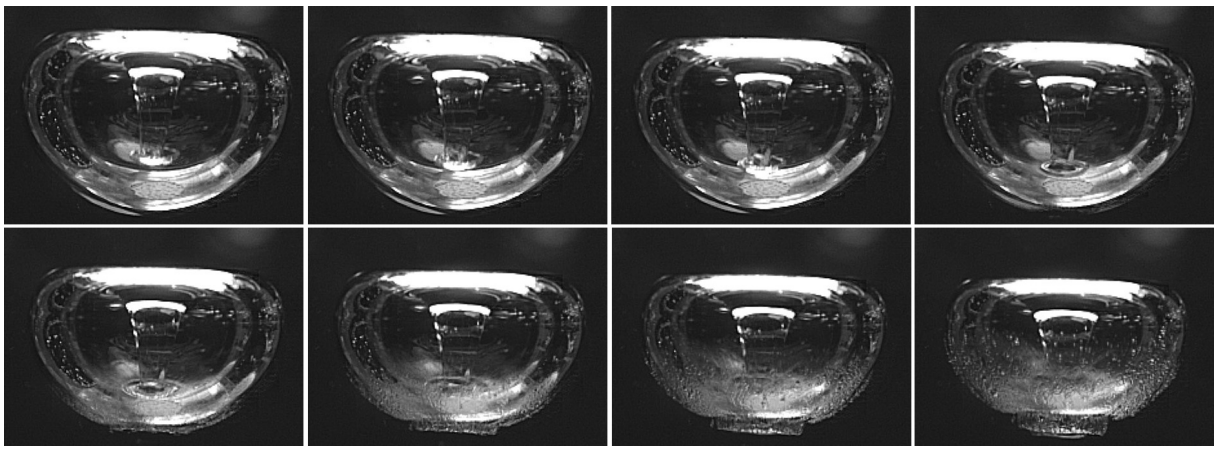

Figure 2: Visualization of jet impact within the collapsing cavitation bubble. First frame taken 2.25 ms after bubble generation. Inter-frame time 26 μs.

the bubble end up covering the entire bubble surface, including the jet. As a consequence, the bubble-jet system becomes less transparent to light and more difficult to observe.

It should be noted that mathematically the bubble maintains a spherical topology, as opposed to a toroidal one, until the vapor jet pocket detaches from the main bubble. At this moment, the bubble separates into two pockets, a torus associated with the main bubble, and a cylindrical pocket, still of spherical topology, associated with the jet (see frame 5 in Figure 1). These two bubble parts collapse individually with the cylindrical part breaking again into tori during its collapse. The initial micro-jet is still present within the rebound bubble, but it is barely visible due to the non-transparent interface of the rebound reminiscent of an upside-down mushroom cloud (frame 6 in Figure 1).

Figure 3 shows the evolution of the bubble radius with time from the bubble generation to

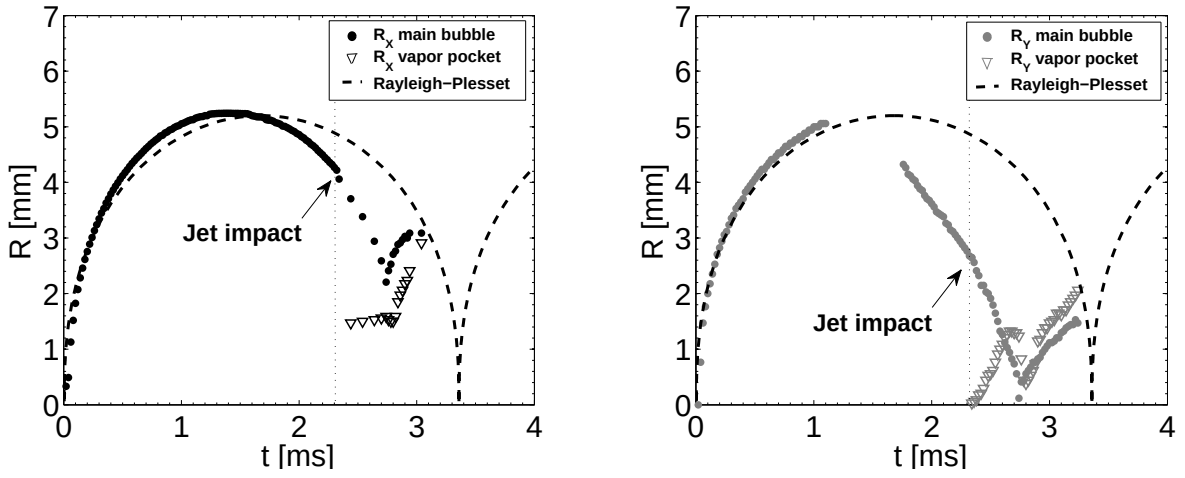

(a) R_X (b) R_Y

Figure 3: Time evolution of bubble radius in (a) horizontal and (b) vertical direction for the main bubble and the vapor pocket, compared with the Rayleigh-Plesset solution for a spherical bubble with $R_{\max} = R_X = 5.25$ mm and $p_\infty = 0.1\text{atm} = 10.15$ kPa, thus $\Delta p = p_\infty - p_{\text{vapor}} = 8.10$ kPa.

its collapse and first rebound. The bubble radius is measured separately in the horizontal (X) and vertical (Y) direction, since the bubble evolves into a shape that is not a sphere. These radii are calculated from the measured diameters, $R_X = D_X/2$ and $R_Y = D_Y/2$. Such a choice allows us to compare the measured bubble size with the Rayleigh-Plesset model describing the radial evolution of a corresponding spherical bubble [9]. In Figure 3b there is a region in time where the exact size of the bubble is difficult to extract due to the bubble being partly covered by the free surface. It is evident that the shrinking of the main bubble is accelerated after the jet impact at $t = 2.32$ ms (see the radius gradient change in Figure 3b), making it collapse faster than the Rayleigh model would predict. This is explained by part of the bubble contents being pushed away by the jet and participating in the growth of the external vapor pocket. The two bubbles collapse individually with a time difference of $\sim 60\mu$s, and the vapor pocket breaks up further during its collapse, releasing several individual tori.

A final feature worth discussing is the low velocity of the jet inside our bubble. We find typical values around 8.2 m/s, which are significantly smaller than usually reported values around 50-150 m/s [8]. This difference is, however, explainable by our low pressure settings of 0.1 atm and the close proximity of the bubble to the free surface, corresponding to a stand-off parameter $\gamma = h/R_{\max} = 0.56$, where h is the distance of the initial bubble centre to the free surface. In fact, empirical models suggest jet velocities around $U_J = \xi(\Delta p/\rho)^{1/2}$ [8], where $\Delta p = p_\infty - p_{\text{vapor}}$ is the driving pressure, ρ is the density of the liquid, and ξ is a constant, numerically found to be around $\xi \sim 2.5$–3 for $\gamma = 0.56$ [10]. Using this constant, we then predict jet velocities of 7.1–8.6 m/s, consistent with our measurements.

3. Conclusion

The dynamics of the micro-jet impact within a laser-generated cavitation bubble collapsing in the vicinity of a free surface has been experimentally studied using high-speed imaging. Low pressure conditions and large bubble energies (obtained with a focussed laser) provide large and slowly moving bubbles and therefore excellent temporal and spatial resolutions to investigate detailed features of the collapse. The "mushroom cap"-shape of the jet tip, the crown-splash forming at the jet impact within the bubble and the micro-droplet shooting on the interface were discovered.

Acknowledgements

We gratefully acknowledge the support of the Swiss National Science Foundation (Grant no. 513234), the European Space Agency, and the support of the University of Western Australia Research Collaboration Award obtained by co-authors DO and MF.

References

[1] Supponen O, Kobel P, Obreschkow D and Farhat M 2015 *Phys. of Fluids* **27** 091101
[2] Obreschkow D, Tinguely M, Dorsaz N, Kobel P, De Bosset A and Farhat M 2011 *Phys. Rev. Letters* **107** 204501
[3] Zhang A M, Cui P and Wang Y 2013 *Exp. Fluids* **54** 1602
[4] Obreschkow D, Tinguely M, Dorsaz N, Kobel P, De Bosset A and Farhat M 2013 *Exp. Fluids* **54** 1503
[5] DOI: http://dx.doi.org/10.1103/APS.DFD.2014.GFM.V0084
[6] Yarin A L 2006 *Annu. Rev. Fluid Mech.* **38** 159-92
[7] Deegan R D, Brunet P and Eggers J 2007 *Nonlinearity* **21** C1
[8] Blake J R and Gibson D C 1987 *Ann. Rev. Fluid Mech.* **19** 99-123
[9] Rayleigh L 1917 *Phil. Magazine* **34** 94-98
[10] Robinson P B, Blake J R , Kodama T, Shima A, and Tomita Y, 2001 *J. Appl. Phys.* **89** 12